Science of the Total Environment 946 (2024) 174468

Contents lists available at ScienceDirect

Science of the Total Environment

journal homepage: www.elsevier.com/locate/scitotenv

Impact of abiotic stressors on nutrient removal and rhizomicrobiome composition in floating treatment wetland with *Equisetum hyemale*

Nicole Nawrot [a,*], Przemysław Kowal [a], Ewa Wojciechowska [a], Ksenia Pazdro [b], Jolanta Walkusz-Miotk [b], Sławomir Ciesielski [c], Filip M.G. Tack [d]

[a] Gdansk University of Technology, Faculty of Civil and Environmental Engineering, Narutowicza 11/12, 80-233 Gdansk, Poland
[b] Institute of Oceanology of the Polish Academy of Sciences, Marine Geotoxicology Laboratory, Powstancow Warszawy 55, 81-712 Sopot, Poland
[c] University of Warmia and Mazury in Olsztyn, Department of Environmental Biotechnology, Sloneczna 45G, 10-917 Olsztyn, Poland
[d] Ghent University, Faculty of Bioscience Engineering, Department of Green Chemistry and Technology, B-9050 Ghent, Belgium

HIGHLIGHTS

- High TN removal in *Equisetum hyemale* floating treatment wetlands (FTW)
- The presence of As suppresses PO_4-P removal
- FTW with *E. hyemale* effectively removes Pb (up to 98 %) and As (up to 79 %)
- Pb treatment reduces bacterial biodiversity and selects *Pseudomonas* and *Azotobacter*.
- Bacterial mediation suggested in removal processes of As

GRAPHICAL ABSTRACT

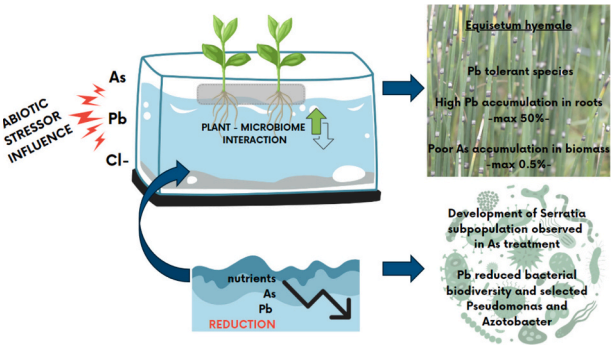

ARTICLE INFO

Editor: Paola Verlicchi

Original content: Floating treatment wetland with Equisetum hyemale - performance in nutrients and potentially toxic elements removal (Original data)

Keywords:
Treatment wetlands
Rhizomicrobiome
Lead
Arsenic
Salinity
Phytoaccumulation

ABSTRACT

Floating treatment wetlands (FTW) are receiving growing interest as a phyto-technology. However, there are significant research gaps regarding the actual role of plant species and plant-microbiome interactions. In this study, the nutrient uptake of *Equisetum hyemale* was examined in FTW microcosms under the influence of abiotic stressors: As (3 mg/L) and Pb (3 mg/L) as well as Cl^- (300 and 800 mg/L) in reference to a control during a short screening experiment. High removal efficiency of nutrients in water solutions, up to 88 % for TN and 93 % for PO_4-P, was observed. However, PO_4-P removal was inhibited in the As reactor, with a maximum efficiency of only 11 %. Lead and As were removed with high efficiency, reaching 98 % and 79 % respectively. At the same time only Pb was effectively bound to root biomass, reaching up to 51 %. Limited As accumulation of 0.5 % in plant roots suggests that microbial processes play a major role in its reduction. The development and structure of microbiome in the microcosms was analysed by means of 16S rRNA gene amplicon sequencing, proving that Pb was the most influential factor in terms of selection pressure on specified bacterial groups. In the As treatment, the emergence of a *Serratia* subpopulation was observed, while the Cl^- treatment preserved a rhizobiome composition most closely resembling the control. This study indicates that *E. hyemale* is a suitable species for use in FTWs treating Pb polluted water that at the same time is capable to withstand periodic increases in salinity.

* Corresponding author.
E-mail address: nicnawro@pg.edu.pl (N. Nawrot).

https://doi.org/10.1016/j.scitotenv.2024.174468
Received 26 February 2024; Received in revised form 25 June 2024; Accepted 1 July 2024
Available online 3 July 2024

E. hyemale exhibits low As binding in biomass; however, extended exposure might amplify this effect because of the slow-acting, but beneficial, mechanism of As uptake by roots and shoots. Microbiome analysis complements insights into mechanisms of FTW performance and impact of stress factors on bacterial structure and functions.

1. Introduction

Anthropogenic-related activities such as expanding industrialization, urbanization, as well as agriculture have disturbed the biogeochemical cycles of nutrients (Geng et al., 2017), leading to rapid increase of nitrogen (N) and phosphorus (P) concentrations in aquatic ecosystems during the last decades. The elevated nutrient loads contribute to the eutrophication as well as impoverishment of aquatic species. At present effective, low-cost and environmentally friendly treatment of lakes, ponds, streams, and rivers supplemented with excessive nutrients still remains a challenge. Apart from nutrient supplementation, water bodies also suffer from inputs of potentially toxic elements (PTEs), mostly heavy metals and arsenic (As), delivered with contaminated surface runoff (Colares et al., 2020). Low-investment nature-based solutions with minimal energy consumption and environmental imprint such as constructed wetlands can mitigate these problems. However, typical constructed wetland systems located near the receiving waters are land demanding, which can be problematic at densely populated sites. In contrast, floating treatment wetlands (FTW), small artificial platforms where macrophytes grow hydroponically, have no specific land requirements and can be easily deployed *in situ* on natural and man-made water bodies (Wang et al., 2019). Plant roots expanding in the water column provide an extensive surface area for the growth of the attached biofilm and entrapment of suspended particulate matter (Borne et al., 2013). The nutrient removal pathways of FTW systems include several biotic and abiotic pathways. The roots suspended in the water column remove nutrients either by incorporating them into their tissues through biosynthesis (both N and P) or by settling (P removal). Microbially driven processes, such as nitrification, denitrification, and anaerobic ammonium oxidation (anammox), mediate N removal in FTW. Pavlineri et al. (2017) point out that nutrient removal varies between research studies in a wide range from 14 to 74 % for N and from 11 to 99 % for P. Hence, the role of plants is worth further exploration with regard to different species and environmental stressors that may stimulate or decrease the phyto-uptake capability, such as PTEs washed off from urban catchments, or elevated concentrations of chloride (Cl^-), a common de-icing agent used in winter on streets under cold and temperate climate. Plant species tolerant to stress factors, capable to maintain high N and P removal, and possibly also capable of taking up PTEs, will be a good selection for FTWs in the urban environment. In general, many plant species demonstrate a high ability to adapt to prevailing environmental conditions, i.e., contamination, pH, salinity, etc. For example, metal-tolerant macrophytes include *Phragmites australis, Lemna minor, Pistia stratiotes*, and *Iris pseudacorus*. However, in each environment, there are more species with unique traits that can be considered in FTW application to increase biodiversity and strengthen the system's abilities to mitigate pollutant concentrations and maintain healthier ecosystems.

Equisetum sp., fern-like plants that can live in both aquatic and land habitats, have been appointed as As and metals hyperaccumulators, capable of accumulation of up to 100,000 mg As/kg d.w. from contaminated soils around mining sites in their tissues (Koch et al., 2022). *Equisetum* (horsetail plants) are commonly found worldwide except Australia and New Zealand. The plants are made of annual and perennial stems that arise from a deep perennial rhizome, and their root system is extensive. *Equisetum* sp. is also highly tolerant to acidic pH, and it is characterized by a high silicate content of the stem (approx. 25 % d.w.). Silicon in plants can affect metal mineralization by solution or solid-state interactions. It also imparts structural, defensive, and photosynthetic advantages to plant systems, and silicon-metal interaction is an important part of their biochemistry. According to Pant et al. (2015) *Equisetum* spp. (including *E. diffusum*) is useful for detoxification of e-wastes containing Pb, while Cannon et al. (1968) reported generally good tolerance of *Equisetum* spp. to heavy metals. To date, apart from the recent study of Koch et al. (2022), who investigated As uptake of three *Equisetum* spp. in hydroponic conditions, no research thus far examined the use of these plants in treatment wetlands. The distinguished ability of *Equisetum* spp. to mediate As contamination can be of potential interest in such systems.

Some recently published studies underline the significance of plant-microbiome synergism as a major driving factor of processes inside FTWs (Yasin et al., 2021). Plant species stimulate the selective development of microbial consortia, while the microbiome supports plants physiological processes and adaptation to environmental stress factors. Still little is known about structure and diversity of microbiome in FTWs, particularly with regard to abiotic stress response. Since microbiome is an integral component of FTW phyto-technology, exploration of the development of microbial consortia under stress factors is of utmost significance and will contribute to understanding its contribution to the overall performance of FTW.

The objective of this study is to assess the impact of stress factors (Pb, As, increased salinity) on the nutrient uptake capacity of *Equisetum hyemale* in FTW microcosms. The ability of *E. hyemale* to uptake Pb and As is also investigated. Additionally, the study aims to identify the structure and diversity of microbial communities in FTW with *E. hyemale* under these stress conditions. The research hypothesis is that *E. hyemale* can be effectively used in hydroponic systems for detoxification of toxic compounds due to its high Si content, which confers multiple benefits on plants, enhancing their structural integrity, defense mechanisms, and photosynthetic efficiency. The findings of this study will contribute to a better understanding of the treatment mechanisms and the role of biotic components of FTWs, and explore the potential of *E. hyemale* as a plant species for removal of Pb and As from water bodies.

2. Materials & methods

2.1. Experiment design

A microcosm experiment was carried out in eight plastic reactors (15 L volume), with the following dimensions: diameter 0.3 m, height 0.31 m, and surface area 0.1 m^2. A floating raft with 5 seedlings of *E. hyemale* 'Robustum' was placed in each reactor (0.03 m^2 of coverage ratio). *E. hyemale* seedlings used in the experiment had a stem approximately 28 cm long and exhibited a rhizome with well-developed roots and branches ranging from 3.6 to 5.8 cm in length. Each seedling had 2–3 stems attached to the rhizome. Before transplanting, each seedling was thoroughly washed with deionized water. Five seedlings were planted in each of the eight reactors, resulting in a similar arrangement of roots and rhizomes with a comparable moist weight (12.5–13.7 g). For the one-week acclimatisation period before the experiment, the reactors were supplied with tap water. The reactors were kept in the semi-controlled laboratory conditions with a constant air temperature of 20 ± 2 °C and artificial lightening (LED grow 10 W; red 660 nm and blue 460 nm light) with photo period 12/12 h.

Following the acclimatisation period, nutrient solutions containing 4.0 mg/L of N and 1.0 mg/L of PO_4-P were added. The experimental setup consisted of the following treatments chloride (NaCl), lead (Pb), arsenic (As), marked further as R_{Cl-}, R_{Pb}, R_{As}, respectively. Nutrient treatments without additional stress factors served as control reactors - R_{cont}.

Nutrient stock solutions were prepared as a mixture of tap water,

ammonium nitrate (NH_4NO_3) and potassium dihydrogen phosphate (KH_2PO_4). To induce stress sodium chloride NaCl, lead(II)nitrate ($Pb(NO_3)_2$) (CAS 10,099–74-8), and arsenic solution (CAS 7440-38-2) were added to specific treatments. The doses of reagents used to prepare specific treatments are presented in Table 1. Citric acid ($C_6H_8O_7$) was used to regulate pH and maintain a slightly acidic environment in all reactors (5.5–6.3) throughout the experiment. The whole experiment lasted 50 days, from March 1st to April 21st, 2021. Due to observed depletion of nutrients, the solutions were entirely replaced after 30 days of experiment. Therefore, the experiment was divided into two phases: 30 days (1st phase) and another 20 days after replenishing nutrient solutions (2nd phase). The initial concentrations for both experimental phases are presented in Table 1.

2.1.1. Sampling

Nutrient concentrations (TN and PO_4-P) were monitored weekly in the 1st phase and every five days in the 2nd phase, resulting in a total 96 analyses across all treatments. On the start and final day of each experimental phase 30 mL of subsample was taken with a volumetric pipette for Pb and As analyses. Plant tissues (shoots and roots) were harvested at the beginning (random selection of 5 seedlings as representative), at the end of the 1st phase (random harvest of several shoots and roots samples from duplicated treatments), and at the end of the 2nd phase (all produced biomass) for As, Pb, N_{Kjel}, and P analyses. Additionally, at the end of the experiment, roots were collected for the analyses of microbial communities and fresh tissues were used for microscopic examination to verify the potential stressors impact on anatomical structure of *E. hyemale*.

2.2. Chemical analyses

2.2.1. Water samples

Acidity (pH) and temperature (°C) were measured using a portable multi-meter (model HQ4300, Hach Lange, USA). The concentrations of TN, PO_4-P, and Cl^- were determined with a spectrophotometer (DR3900, Hach Lange, USA) according to EN ISO 11905-1, EN ISO 6878, and iron (III) thiocyanate method. Liquid samples for Pb were collected with a syringe, filtered through Millipore filters (0.45 μm), and stored at 8 °C in polypropylene tubes to which 100 μL of 65 % HNO_3 (Suprapur, Merck) per 10 mL was added. Pb content in liquid samples was determined using ICP-MS (Perkin–Elmer, ELAN 9000, USA). Quality control was ensured by analyzing subsamples prepared from the Pb standard (with an initial concentration of 10,000 mg/L) and "blanks", according to the same procedure. Recoveries ranged from 92 to 103 %. The precision, expressed as relative standard deviation, ranged from 3 to 5 %. Liquid samples for As were filtered through Millipore filters (0.45 μm) and stored frozen in polypropylene tubes after collection. From the defrosted sample, 10 mL of subsample (original or diluted depending on the estimated As content) was taken for analysis. Subsequently 1.25 mL of 30 % HCl (Suprapur, Merck) and 1 mL of 20 % KI (EMSURE grade) solution was added in order to ensure conversion of the arsenic to As (III). Arsenic was measured using hydride atomic absorption spectrometer (AAS, Shimadzu 6800, Japan), equipped with a HVG-1 hydride vapor generator (Shimadzu, Japan) with deuterium background correction. Arsenic was determined at a wavelength of 193.7 nm. Recoveries ranged from 93 to 112 %. Precision, given as relative standard deviation, was in the range of 3 to 5 %.

2.2.2. Plant material

N_{Kjel} was determined using semi-automatic Kjeldahl distillation (Behrotest S4, Behr Labor-Technic, Germany). Approximately 0.2 g of plant material was added to 250 mL glass tubes, and 2.4 mL of H_2SO_4, and Kjeldahl tabs Missouri (5 g/tablet, Supelco, Merck) were added. Then the mixture was heated in a heating block (Behrotest, behr Labor-Technic, Germany), gradually increasing the temperature to 380 °C (Table S.1). After cooling the samples were turned alkaline by adding 30 % NaOH water solution (approx. 30 mL) and subjected to steam distillation according to the standard procedure for N_{Kjel} determination (Chemat et al., 1998).

P was determined with the use of the molybdenum blue method (APHA, 4500 PE) as a PO_4-P and determined spectrophotometrically at 690 nm with Tecan GENios Microplate Reader (Tecan Group Ltd., Switzerland). Specific description is attached in Table S.1.

For As determination 0.1 to 2 mL of the solution, depending on As concentrations in the sample, was transferred into polyethylene test tube and diluted with Milli-Q to the volume of 10 mL. Then 1.25 mL of 30 % HCl (Suprapur, Merck) and 1 mL of 20 % KI (EMSURE grade) solution was added so As could be reduced into one oxidation state – As(III). Measurements with AAS equipped with a deuterium background corrector and a HVG-1 hydride vapor generator (Shimadzu, Japan) were proceeded after 30 min and each sample was analysed in triplicate. The operating parameters for working element were set as recommended by the manufacturers. The Pb concentrations were measured in inductively coupled plasma mass spectrometry (ICP-MS, Perkin Elmer 9000 Sciex., USA). To ensure the quality of the results, the same procedure was applied to certified reference material of plant LGC7162 (strawberry leaves), whose As content is 0.28 ± 0.07 mg/kg and Pb content is 1.8 ± 0.4 mg/kg. The obtained results of CRM were 0.262 ± 0.04 and 1.95 ± 0.03 mg/kg respectively for As and Pb, and as such in good agreement with the certified values (recoveries 93.5 and 108 %, respectively). All

Table 1
Initial properties of synthetic wastewater in microcosm reactors at the beginning of 1st and 2nd phases. Control reactor (R_{cont}), chloride treated reactor (R_{Cl-}), lead treated reactor (R_{Pb}), and arsenic treated reactor (R_{As}).

Initial physiochemical properties of synthetic wastewater												
Element	TN [mg/L]		PO4-P [mg/L]		Cl- [mg/L]		Pb [mg/L]		As [mg/L]		pH* [−]	
Phase	1st	2nd	1st	2nd	1st	2nd	1st	2nd	1st	2nd	1st	2nd
R_{cont}	4.0 ± 0.1		1.0 ± 0.1		101 ± 3	313 ± 10	0.0002		0.03		6.1	5.5
R_{Cl-}	4.0 ± 0.1		1.0 ± 0.1		278 ± 5	820 ± 8**	0.0002		0.03		6.3	5.6
R_{Pb}	4.0 ± 0.1		1.0 ± 0.1		105 ± 2	292 ± 2	3.0 ± 0.2		0.03		6.2	5.5
R_{As}	4.0 ± 0.0		1.0 ± 0.1		102 ± 2	299 ± 1	0.0002		3.0 ± 0.1		6.1	5.6

Explanation:
R_{cont} – control reactor, R_{Cl-} - reactor with additional Cl^- dose, R_{As} – reactor with additional As dose, R_{Pb} – reactor with additional Pb dose, 1st phase duration: 1–31 March (30 days), 2nd phase duration: 1–21 April (20 days).
* pH was regulated systematically (every 2 days) with the use of citric acid $C_6H_8O_7$ (2–5 drops)
** value determined basing on the concentrations observed in stormwater retention ponds (Schück and Greger, 2022)

elements concentrations in plants and sediments were reported on a dry weight (d.w.) basis.

2.3. Plant characteristics

Plant height was measured, and the external appearance of plants was inspected once a week, to detect possible senescence. Plants in the FTW basket were lifted above the water level and measured using a portable cm measure. The minimum and maximum range [cm] were recorded. The chlorophyll content index (CCI) was determined using a portable chlorophyll meter (CCM-200 Plus, Opti-Sciences, USA), which provides non-destructive measurements of plants during their growth and cultivation. One sample consisted of a 0.7 cm^2 leaf apex. CCI values were determined using the exact same shoot from the same plants above the last node. The measurements were carried out to avoid damaging the elastic structure of the stems. Measurements were taken for each replicate of each treatment following the methodology proposed by Higbie et al. (2010) and Ling et al. (2011).

2.3.1. Microscope observation

Plant tissues were cut into semi-thin (0.5–1 mm) slices and placed in a watch glass filled with redistilled water (Milli-Q Ultrapure Water System, Merck). After soaking in water for 2–3 min, the cross-sections were immersed in the staining solution for one minute. To distinguish between tissue structures, toluidine blue was used (Parker et al., 1982). After staining, sections were washed in redistilled water, placed on a clean glass slide with a drop of water, and covered with a coverslip. A light microscope (Biolar, PZO Poland) was used to examine cross-sections of roots, stems, and leaves at 5× and 10× magnification of lens and 10× magnification of eyepiece.

2.3.2. Relative growth rate

The relative growth rate (RGR) was calculated considering the initial and final plant heights, according to Eq. (1) as described by Gao et al. (2018):

$$\mathrm{RGR} = 100\frac{ln(H_2/H_1)}{T_2 - T_1}\left[\frac{\%}{\mathrm{day}}\right] \quad (1)$$

where H_1 and H_2 are the initial and final plant heights (cm), respectively, and $(T_2 - T_1)$ is the experimental period (days).

2.4. Microbial analyses

2.4.1. DNA extraction and high-throughput 16S rDNA sequencing

Samples for microbiological analyses were taken at the end of the 2nd phase of the experiment, by cutting off part of the rhizosphere of *E. hyemale* derived from each reactor. The 2–3 cm slices of roots and rhizomes with attached biofilm, obtained from each plant in a given microcosm were packed into single 30 mL polypropylene flask until filly filled with loosely packed tissue fragments. The DNA extraction from the microbial communities developed on plant roots was performed by using 1 g of root tissue sample with the FastDNA™ SPIN KIT (MP Biomedicals, USA) following the manufacturer's protocol. Genomic DNA isolation was carried out in duplicate from each sample. After the extraction step, the genomic DNA solutions from repetitions were combined.

After quality control by spectrophotometry, genomic DNA was subjected to high-throughput Illumina sequencing of the V3-V4 region of the 16S rRNA gene, using the primer set proposed by (Klindworth et al., 2013). The MiSeq sequencing platform (Illumina, USA) using the MiSeq Reagent Kit V2 according to the manufacturer's protocols was used to perform paired-end, 2 × 250 nt sequencing reactions (at sequencing depth with >60,000 reads per sample). The Usegalaxy platform (https://usegalaxy.org) was used to join paired-end reads, filter DNA sequences by quality (Phred score ≥ 20) and length (≥ 100 bp) and perform final quality control using the FastQC tool. After additional checking of chimeras using the online Decipher tool (www2.decipher.codes/FindChimeras.html), DNA sequences were classified at each taxonomic level using the SILVA server (www.arb-silva.de), as described in the earlier work (Kowal et al., 2022).

The sequencing data sets were submitted to GenBank (National Center for Biotechnology Information, U.S.A) to allow public access under submission numbers SUB14194396, SUB14194469, SUB14194475, and SUB14151478.

2.5. Statistical data treatment

Competitive analysis of the bacterial community structure after exposure to As, Pb, Cl and in the control reactor was performed using the Statistical Analysis of Metagenomic Profiles (STAMP v. 2.1.3) software (Parks and Beiko, 2010) by performing an ANOVA test followed by a Tukey-Kramer post-hoc test at a significance level of 95 % ($p < 0.05$) and visualised as a Principal Component Analysis (PCA) plot. Additionally, bacterial communities were characterized in terms of the biodiversity assessed with the Shannon's (H) and Simpson's (D) diversity indices calculated by the following formulas (2,3):

$$H = -\sum_{i=1}^{R} p_i ln p_i \quad (2)$$

$$D = 1 - \sum_{i=1}^{R} p_i^2 \quad (3)$$

where p_i is the ratio between the number of DNA sequences assigned to the particular i^{th} genus to the total number of DNA sequences obtained from the sample. The derived values of Shannon and Simpson indices were independently used to calculate the mean and standard deviation (SD) to determine the statistical significance in bacterial community diversity between the analysed microcosms.

A minimum, maximum, and average value for nutrients, Pb, and As concentration in liquids were determined. The results are presented as the means ± standard error (SE) of three measurements. The concentrations of Pb, As, N_{Kjel}, PO_4-P in plant material were measured in homogenised and mixed samples of harvested biomass from randomly selected plants (in duplicates). The analysis of variance (ANOVA) was run using SPSS (ver. 27, NY, USA) to examine the effects of different treatments on studied species and elements accumulation at a significance level of 95 % ($p < 0.05$) followed by the Tukey honestly Significant Difference (HSD) test.

2.6. Removal and plant accumulation calculations

The removal efficiency (RE; %) of nutrients in the FTW system was estimated using the difference in initial (C_{in}) and final (C_f) concentration (4):

$$\mathrm{RE} = \left(C_{in} - C_f\right)\cdot 100\ [\%] \quad (4)$$

The removal rate (*RR*; mg/m^2/d) was estimated as the difference initial (C_{in}) and final (C_f) concentration divided by FTW_{area} (0.03 m^2) and divided by time of exposure (T_{exp}) (5).

$$\mathrm{RR} = \frac{C_{in} - C_f}{FTW_{area}\cdot T_{exp}}\left[\frac{mg}{m^2\cdot d}\right] \quad (5)$$

Nutrients, Pb and As accumulation (mg) was calculated by multiplying the element concentration in plant dry biomass (ppm; mg/kg d.w.; μg/g d.w.) with dry biomass (g). Accumulation at the end of the 1st phase of the experiment was estimated using the growth parameters of *E. hyemale* and the percentage growth increase of shoots and roots in relations to the initial growth parameters. Shoot and root growth in each reactor was measured using measuring tape to determine min-max ranges. Mass balance calculation strategy of Pb and As in reactors with FTW included determination of (1) Pb and As total content [mg] in

water solution in reactors at the beginning of the 1st and 2nd phase, (2) accumulation of Pb and As in plant tissues (shoots and roots) at the end of the 1st and 2nd phase, (3) Pb and As left in water solution at the end of the 1st and 2nd phase, and (4) Pb and As removed by "other processes" at the of the 1st and 2nd phase. In this approach, "other processes" could mean removing Pb and As (1) from roots through washing before drying harvested plant biomass, (2) related to microorganisms and suspension deposited on the 0.45 μm filter, and (3) precipitating or sorbed on the reactor walls/bottom.

3. Results

3.1. Nutrient removal

During the 1st phase of the experiment the removal efficiency (RE) of TN was from 75 % in R_{Cl^-} to 88 % in R_{As} (Fig. 1) with 79 % achieved in R_{cont}. The percent removal in the initial period was the highest for R_{Pb} and R_{As} resulting in the same highest removal rates (RR) of 3.6 and 3.8 mg/m^2/day, respectively (Table 2). In the case of PO_4-P significant disparities in removal efficiency are observed; it was only 11 % for R_{As} and 93 % for R_{Pb} with 64 % for R_{cont}. It can also be observed that during the first 24-days, the decrease in dissolved PO_4-P in R_{cont} and R_{Cl^-} was small (14 and 34 %, respectively), whereas in the case of R_{Pb}, PO_4-P sharp depletion began after 7 days. Further decrease of PO_4-P concentration was observed after 24 days till the end of the 1st phase (30 day). The average RR (in mg/m^2/day) for PO_4-P in the 1st phase dropped as follows: 1.0 for R_{Pb}; > 0.9 for R_{Cl^-}; > 0.7 for R_{cont}; and > 0.1 for R_{As}.

Following solution renewal in the 2nd phase of the experiment, nutrient removal efficiencies were comparable to those achieved in the 1st phase. Nitrogen RR ranged from 3.6 in R_{As} to 4.5 mg/m^2/day in R_{Pb}. P-PO_4 depletion was the fastest for R_{Pb} (65 %; RR = 1.0 mg/m^2/day), but also observed in R_{cont} (35 %; RR = 0.5 mg/m^2/day) and R_{Cl^-} (38 %; RR = 0.6 mg/m^2/day). On the other hand, during the 2nd phase PO_4-P in R_{As} was virtually unchanged.

3.2. Uptake and translocation in plant tissues

N_{Kjel} and PO_4-P concentrations increased in plant tissues during both

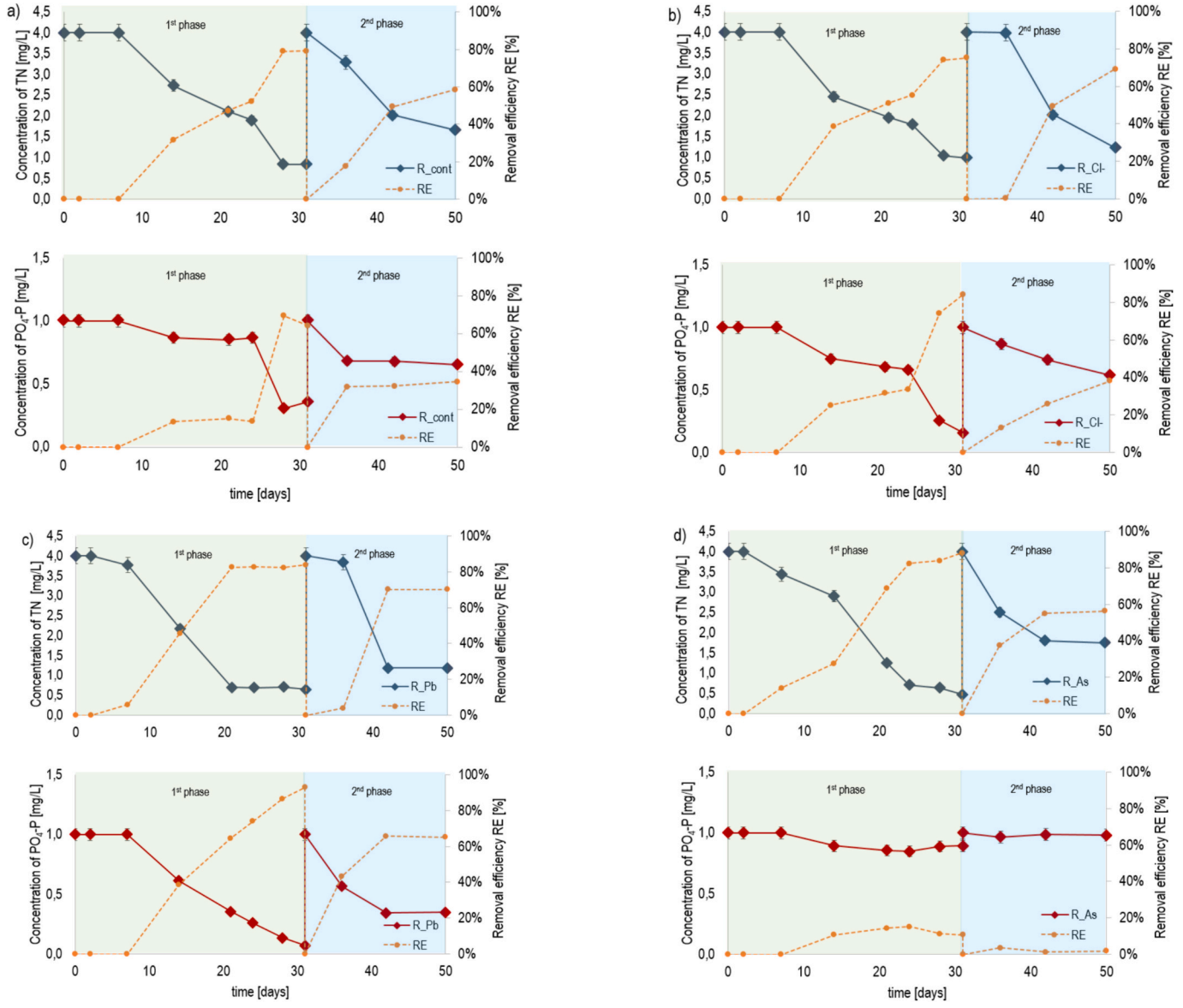

Fig. 1. Changes in TN and PO_4-P concentrations (uncertainty intervals ±10 %) and removal efficiencies in a) R_{cont}, b) R_{Cl^-}, c) R_{Pb}, and d) R_{As} treatments during two phases of the experiment (1st and 2nd phases). Control reactor (R_{cont}), chloride treated reactor (R_{Cl^-}), lead treated reactor (R_{Pb}), and arsenic treated reactor (R_{As}), removal efficiency (RE), total nitrogen (TN), orthophosphate phosphorus (PO_4-P).

Table 2
Concentrations of N_{Kjel}, PO_4-P, Pb and As in plant biomass, Pb and As in liquids at the beginning and end of two subsequent phases of the experiment. Control reactor (R_{cont}), chloride treated reactor (R_{Cl-}), lead treated reactor (R_{Pb}), and arsenic treated reactor (R_{As}). Superscript letters indicate significant differences among treatments for each species at $p < 0.05$.

Parameter/ part of plant phase of experiment	Unit	Reactor			
		R_{cont}	R_{Cl-}	R_{Pb}	R_{As}
N_{Kjel}†					
shoots 1st phase start		8.5 ± 0.25[a]			
shoots 1st phase end/ 2nd phase start		9.4 ± 0.28[a]	10.9 ± 0.33[b]	12.6 ± 0.38[c]	11.5 ± 0.35[b]
shoots 2nd phase end		14.1 ± 0.42[a]	13.6 ± 0.41[ab]	13.1 ± 0.39[b]	13.4 ± 0.40[b]
roots 1st phase start		13.2 ± 0.40[a]			
roots 1st phase end/ 2nd phase start		13.2 ± 0.40[a]	13.8 ± 0.41[ab]	14.2 ± 0.43[b]	14.1 ± 0.42[b]
roots 2nd phase end	g/kg	13.8 ± 0.41[a]	14.5 ± 0.44[b]	22.9 ± 0.69[c]	15.6 ± 0.47[b]
PO_4-P†					
shoots 1st phase start		0.89 ± 0.07[a]			
shoots 1st phase end/ 2nd phase start		1.38 ± 0.11[ab]	1.22 ± 0.10[bc]	1.46 ± 0.12[a]	1.12 ± 0.09[c]
shoots 2nd phase end		1.45 ± 0.12[ab]	1.54 ± 0.12[ab]	1.63 ± 0.13[a]	1.35 ± 0.11[b]
roots 1st phase start		0.56 ± 0.05[a]			
roots 1st phase end/ 2nd phase start		1.56 ± 0.12[a]	1.42 ± 0.11[a]	1.98 ± 0.16[b]	0.88 ± 0.07[c]
roots 2nd phase end	g/kg	1.6 ± 0.13[a]	1.65 ± 0.13[a]	2.11 ± 0.17[b]	1.01 ± 0.08[c]
Pb and As in liquids					
1st phase start		Pb – 0.0002[a]/ As – 0.03[a]	–	3.1 ± 0.3[b]	3.05 ± 0.1[c]
1st phase end/ 2nd phase start	mg/ L	Pb – 0.0002[a]/ As – 0.03[a]	–	0.06 ± 0.01[b]/ 3.0 ± 0.2[b]	0.65 ± 0.04[c]/ 3.01 ± 0.08[c]
2nd phase end		Pb – 0.0002[a]/ As – 0.03[a]	–	0.23 ± 0.02[b]	0.78 ± 0.05[c]
Pb plant material					
shoots 1st phase start		1.3 ± 0.5[a]			
shoots 1st phase end/ 2nd phase start		1.77 ± 0.5[a]	–	57.7 ± 1.1[b]	–
shoots 2nd phase end		1.91 ± 0.6[a]	–	89.2 ± 1.8[b]	–
roots 1st phase start		11.4 ± 5.6[a]			
roots 1st phase end/ 2nd phase start		8.14 ± 3.1[a]	–	3203 ± 2[b]	–
roots 2nd phase end	mg/ kg	9.22 ± 4.6[a]	–	4901 ± 5[b]	–
As plant material					
shoots 1st phase start		0.07 ± 0.06[a]			
shoots 1st phase end/ 2nd phase start		0.19 ± 0.07[a]	–	–	11 ± 2.3[b]
shoots 2nd phase end		0.22 ± 0.1[a]	–	–	20.3 ± 1.8[b]
roots 1st phase start		0.28 ± 0.1[a]			
roots 1st phase end/ 2nd phase start		0.17 ± 0.1[a]	–	–	25.4 ± 2.7[b]
roots 2nd phase end	mg/ kg	0.34 ± 0.1[a]	–	–	48.1 ± 2.1[b]

†N_{Kjel} – Kjeldahl nitrogen [g/kg], PO_4-P – orthophosphates [g/kg]

phases of the experiment (Table 2). Although it is widely recognized that nutrients usually accumulate in aerial parts of higher plants (Marschner, 2012), in this study N_{Kjel} and PO_4-P concentrations in *E. hyemale* were greater in roots than in shoots. The exception was R_{As}, where PO_4-P concentration was higher in shoots than in roots. R_{cont}, R_{Cl-}, and R_{As} showed similar results for N_{Kjel} in shoots and roots at the end of both phases of experiment. In contrast, in R_{Pb}, N_{Kjel} concentration was approximately 1.5 times higher at the end of the 2nd phase in comparison to the 1st phase. The different uptake pattern in this reactor could be associated with observed effects of Pb addition on microbiome structure, which is further discussed.

Pb removal efficiency (RE) in R_{Pb} reached 98 % at the end of the 1st phase, and 92 % at the end of the 2nd phase (Table 2, Fig. 2a). Pb concentration in shoots increased from 1.3 ± 0.5 mg/kg d.w. to 57.7 ± 1.1 mg/kg d.w. (44 times) by the end of the 1st phase and to 89.2 ± 1.8 mg/kg d.w. (69 times) by the end of the 2nd phase. At the same time, Pb concentrations increased in roots reaching 3203 ± 2 mg/kg d.w. (28 times) by the end of the 1st phase and 4901 ± 5 mg/kg d.w. (43 times) by the end of the 2nd phase. Translocation of Pb from roots to shoots was rather poor (at the end of the 1st and 2nd phase shoot/root ratio: 0.02), which is confirmed by observations reported in other studies (Liu et al., 2023). According to a mass balance (Fig. 2a) 50 % of Pb at the end of the 1st phase and 32 % of Pb at the end of the 2nd phase were bound in roots. Shoots were responsible for 1 % Pb accumulation at the end of both phases. Still about 47 % of Pb in the 1st phase and 60 % of Pb in the 2nd phase were subjected to removal by other processes.

As was removed with 79 % and 74 % efficacy during 1st and 2nd phase, respectively, which is similar to the findings demonstrated by Koch et al. (2022) who reported the removal efficiency in the range 53–78 % for different *Equisetum* sp. in 1 mg/L treatment, with *E. hyemale* achieving a range of 69–71 %. The As concentration in roots increased from 0.28 ± 0.1 mg/kg d.w. to 25.4 ± 2.7 mg/kg d.w. at the end of the 1st phase and to 48.1 ± 2.1 mg/kg d.w. at the end of the 2nd phase. These results demonstrate capability of As uptake by *E. hyemale*. However, the percentage accumulation of As in plant tissues was very poor, achieving 0.2 % for shoots and 0.5 % for roots at the end of both phases, in accordance with the mass balance (Fig. 2b).

3.3. Development of *E. hyemale* under abiotic stress in FTW reactors

E. hyemale demonstrated growth of both aerial and underwater parts during the experiment (Fig. 3). The RGR for shoots during 1st phase was between 0.07 and 0.15 % per day and during 2nd phase between 0.06 and 0.21 % per day. For roots the highest RGR was observed for control. Remarkably, RGR = 0.41 % per day for roots in R_{As} during the 1st phase suggests that As dosage had no adverse effect on *E. hyemale* growth. In general, *E. hyemale* grows up to 90 cm in the wild (Walkowiak, 2018). During the experiment, the plants were approx. 30 cm high. It should however be noted that the experiment duration was short: it lasted for only 50 days outside the flowering season. The morphometric parameters for shoots and roots were similar for control, salinity, and As treatments. A different pattern (faster growth of shoots and roots) was achieved by *E. hyemale* in R_{Pb}.

Chlorophyll content index (CCI) (Table 3) in all reactors decreased with time. No significant differences were observed between treatments. The decrease of CCI during the experiment may suggest that artificial conditions affected the photosynthesis process. In other studies (Mohsin et al., 2023; Yang et al., 2020) a increase of CCI with increased dosage of Cd and Pb was demonstrated for *Phragmites australis, Iris pseudacorus*, and *Davidia involucrate*. On the other hand, Spinedi et al. (2019) found that CCI decreased with increasing anthracene concentrations in *Marchantia polymorpha*. The diminishing trend of CCI could be associated with a decrease in a specific plant's susceptibility to the cultivation conditions.

Internode cross sections of rhizome and aerial stem, both made of the outermost layer – epidermis (Ep), with silica deposits in their outer and lateral walls, are depicted in Fig. 4.a-b. Between Ep and endodermis (En) the outer and inner regions of cortex (Cortx) are visible in all treatments (Fig. 4a). The central area of the rhizomes and aerial shoot's internode is occupied by a huge pith cavity (PC) generated by fast extension of the internodal region. Vallecular canals (VC) and vascular bundles (carinal canal, CC) are arranged alternate in a ring. In R_{Pb} rhizomes disturbances

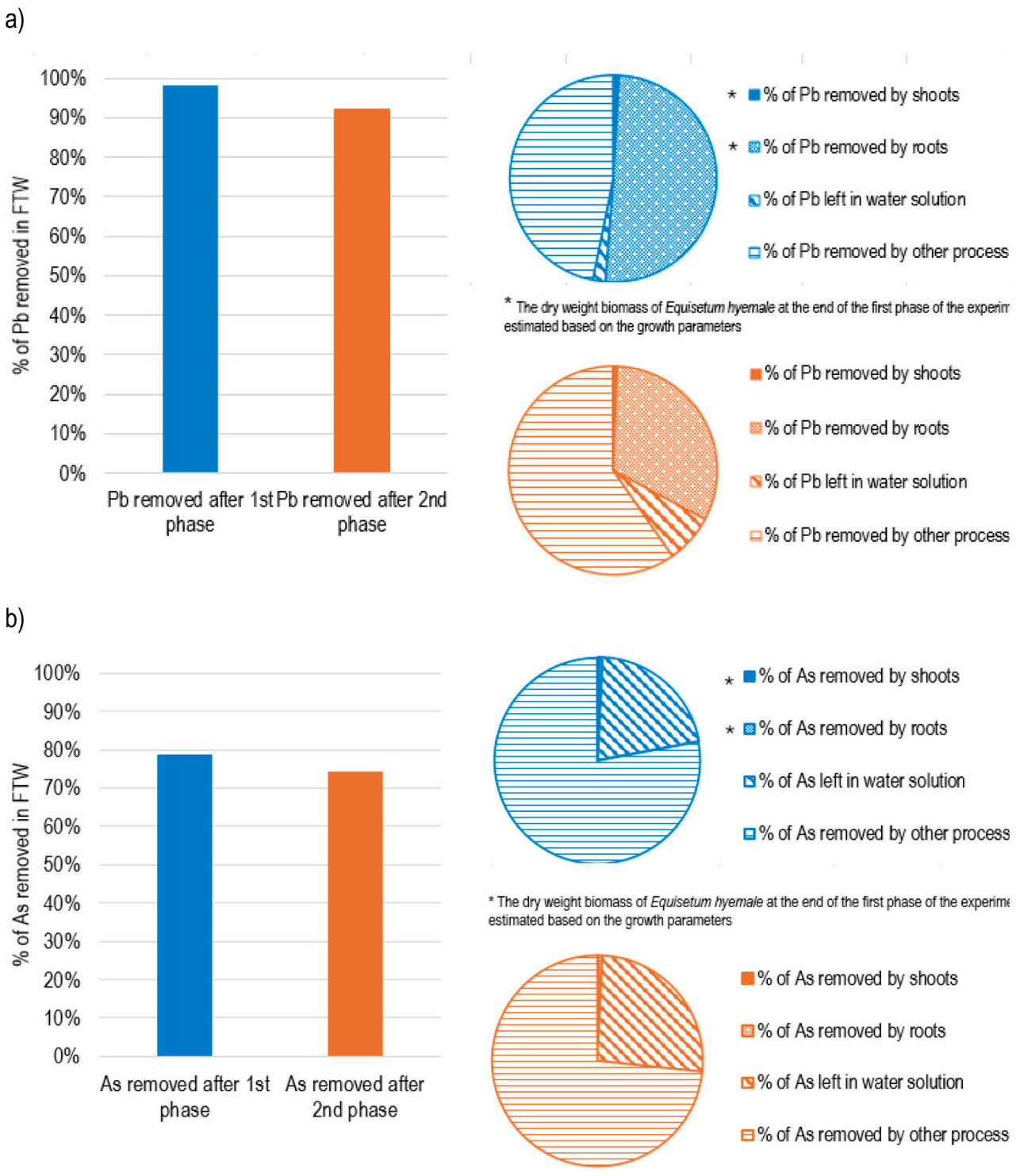

Fig. 2. Removal efficiency of a) Pb and b) As in floating treatment wetlands with *E. hyemale* and percentage mass balance of each element at the end of the 1st and 2nd phase of the experiment.

in a septum are visible (marked with a red arrow); it appears to be VC formation, with two CC visible fairly irregularly formed. VC are elongated in the Cortx of R_{As}, reaching from Ep to En, while CC are organized regularly. Aerial stem cross section (Fig. 4b) is wavy in outline because of the presence of ridges and grooves. A large patch of sclerenchyma, mechanical in function, is located just below each ridge. The chlorenchyma is represented by the green colour. Sc is also found beneath the grooves between the chlorenchyma. In general, aerial stems in all treatments are arrange on similar way; the only exception is R_{Pb}, where CC formation is irregular.

3.4. Structure and diversity of the bacterial communities

After quality control, a total number of 333,499 DNA sequences of the 16S rRNA gene fragment were obtained. Considering the samples from a given reactor, the following numbers of amplicons were obtained: R_{cont} – 76,102, R_{Pb} – 86,936, R_{As} – 79,206, R_{Cl} – 91,255. The averaged G + C content within the DNA sequence data sets analysed was

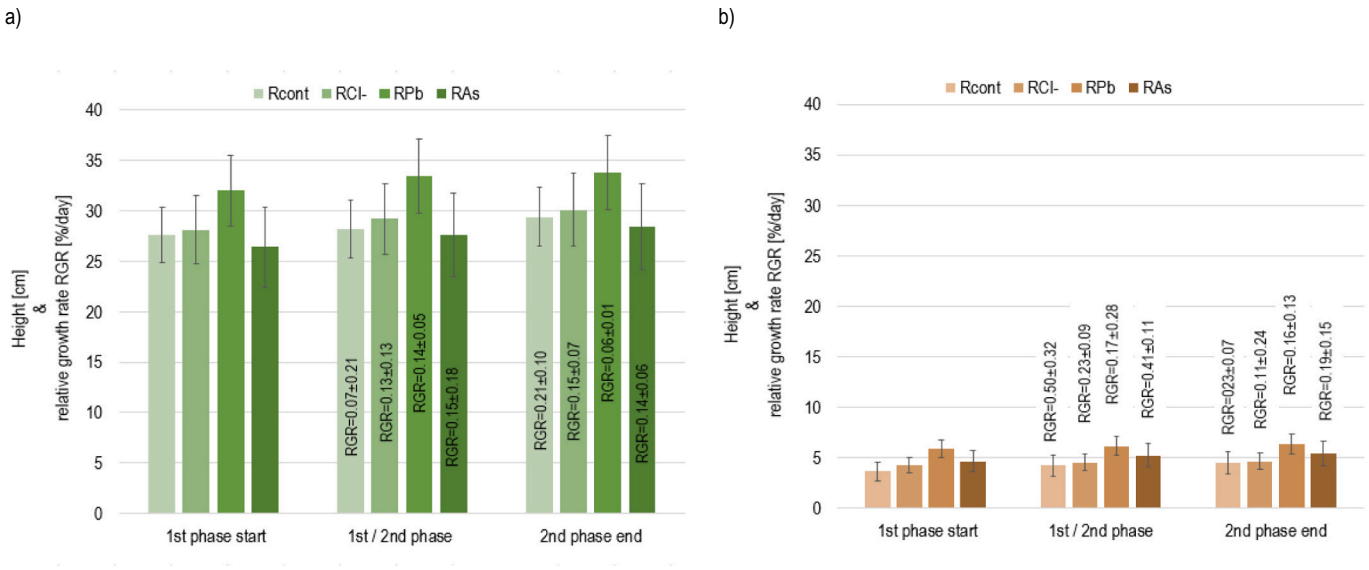

Fig. 3. *E. hyemale* growth parameters of a) shoots and b) roots at different stages of the experiment and relative growth rate RGR [%/day] in R_{cont}, R_{Cl-}, R_{Pb}, and R_{As}. Control reactor (R_{cont}), chloride treated reactor (R_{Cl-}), lead treated reactor (R_{Pb}), and arsenic treated reactor (R_{As}).

Table 3
Heat map of the relative abundance of the specified bacteria taxa in the total bacterial community at the genus level. Percentage identity of DNA sequences with 16S rRNA sequences of the currently characterized genera was the main criterion for taxonomic assignment. In terms of heatmap colours from white (0 %) to intensive red (25 %) corresponds to low and high standardized relative abundance values, respectively. Colours in the metabolic features correspond to the: widely recognized dominant metabolic model (green) and potential and/or facultative (yellow).

R_{cont}	R_{As}	R_{Cl}	R_{Pb}	BLAST/MiDAS 4.8.1 closest relative genera	Per. Ident	Predominant metabolism	Ammonium oxidizing bacteria	Nitrite oxidizing bacteria	Sulfate reduction	Fermentation	Nitrite reduction	Sugars	Proteins/ amino acids
4.7%	2.5%	2.7%	1.2%	*Nakamurella*	99.0%	Aerobic heterotroph							
4.5%	2.0%	3.2%	24.4%	*Pseudomonas sp.*	98.8%	Aerobic heterotroph							
3.9%	6.2%	7.8%	4.8%	*Mycobacterium*	99.8%	Aerobic heterotroph/chemoautotroph							
3.6%	1.4%	2.9%	1.1%	*Nocardioides*	96.1%	Aerobic heterotroph							
2.6%	2.6%	2.4%	0.4%	*Limnohabitans*	99.8%	Aerobic heterotroph							
2.4%	0.8%	0.9%	0.1%	*Rhodoferax*	99.3%	Aerobic heterotroph							
2.1%	4.7%	3.4%	2.7%	*Rhodobacter*	97.0%	Aerobic heterotroph/chemoautotroph							
2.1%	3.3%	1.3%	0.8%	*Bradyrhizobium*	96.5%	Aerobic heterotroph/chemoautotroph							
1.9%	0.7%	1.2%	0.3%	*Variovorax*	98.6%	Aerobic heterotroph/chemoautotroph							
1.8%	2.3%	2.3%	0.4%	*Rubrivivax*	98.3%	Aerobic heterotroph/chemoautotroph							
1.7%	0.3%	0.6%	0.0%	*Hydrogenophaga*	99.3%	Aerobic heterotroph/chemoautotroph							
1.6%	1.7%	1.7%	5.5%	*Aestuariivirga*	92.4%	Not defined							
1.5%	1.8%	2.3%	0.8%	*Allorhizobium-Neorhizobium-Pararhizobium-Rhizobium*	100.0%	Aerobic heterotroph							
1.4%	0.7%	2.2%	0.0%	*Massilia*	97.6%	Not defined							
1.1%	0.8%	1.5%	0.2%	*Pirellula*	99.3%	Aerobic heterotroph							
1.1%	1.8%	1.5%	0.9%	*Reyranella*	96.6%	Aerobic heterotroph							
0.9%	1.2%	2.0%	3.1%	*Devosia*	99.0%	Heterotroph							
0.4%	0.7%	0.5%	0.8%	*Nitrosomonas*	90-92%	Chemoautotroph/mixotroph							
0.3%	0.6%	1.3%	0.1%	*Chthoniobacter*	93.1%	Not defined							
0.2%	0.2%	0.1%	0.1%	*Nitrospira*	99.8%	Chemoautotroph/mixotroph							
0.2%	0.2%	0.4%	2.0%	*Pseudomonas poae*	91.9%	Aerobic heterotroph							
0.1%	0.1%	0.0%	1.2%	*Saprospiracea_midas_g_729*	99.8%	Heterotroph							
0.04%	0.02%	0.02%	0.02%	*Nitrosopira*	100.0%	Chemoautotroph/mixotroph							
0.0%	0.1%	0.1%	1.0%	*Afifella*	92.6%	Heterotroph							
0.0%	0.4%	0.2%	10.7%	*Azotobacter*	98.6%	Aerobic heterotroph							
0.0%	0.8%	0.0%	0.0%	*Serratia*	99.5%	Aerobic heterotroph							

54 ± 4 %. PCA analysis showed variation in bacterial community composition between the experimental reactors (Fig. 5a). The most similar bacterial rhizobiome composition in relation to control was noted for R_{Cl}, then for R_{As}. The bacterial community in R_{Pb} was noticeably different from the others. This suggests that Pb, at the concentrations applied, was the most influential factor in terms of selection pressure on specified bacterial groups.

Rarefaction curve analysis confirmed sufficient sampling coverage of the analysed amplicons sets (Fig. 5b). The highest normalized OTU richness per 1000 reads was noted for R_{As} (102 OTUs), then R_{Cl-} (93 OTUs), R_{cont} (84 OTUs), and the lowest for the R_{Pb} (78 OTUs). The values of the Shannon index were at comparable levels for R_{As}, R_{Cl-}, R_{cont} and ranged from 4.93 to 5.10 (in relation to the mean value from all analysed cases 4.76 ± 0.50), while it was significantly lower for R_{Pb}, whose value

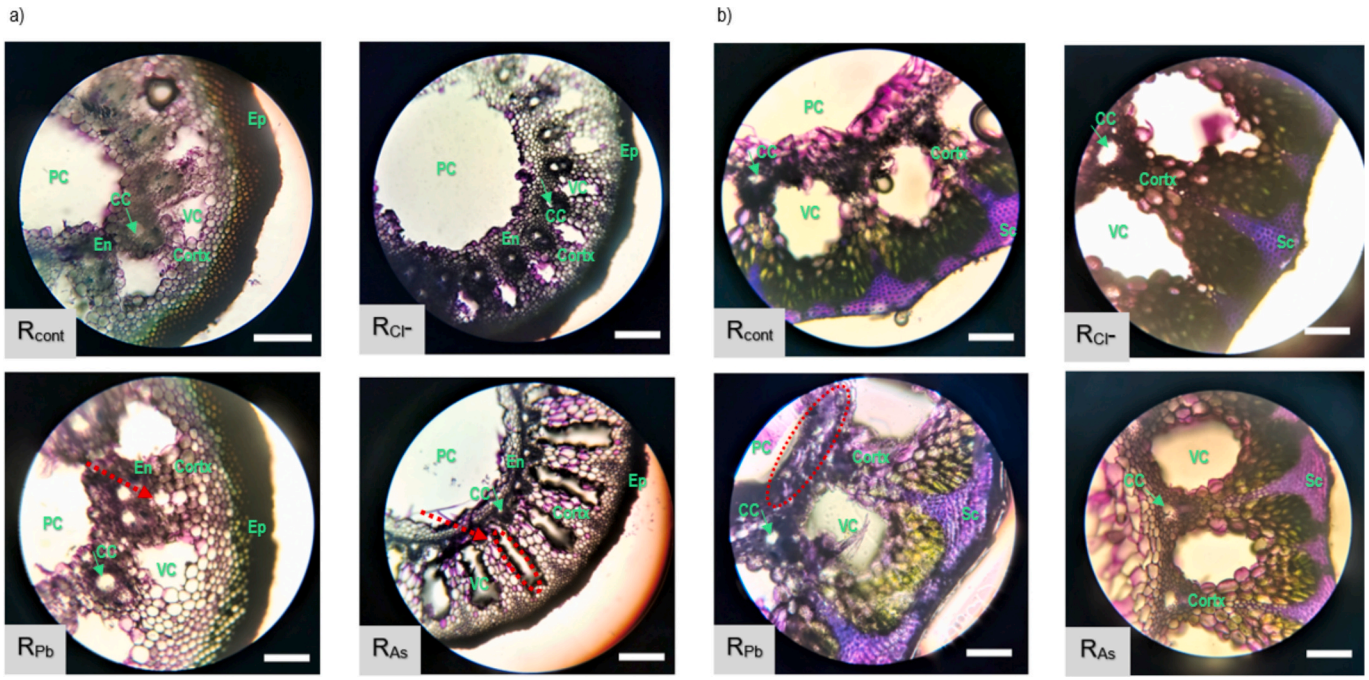

Fig. 4. *E. hyemale* cross section of an internode of a) rhizome and b) aerial stem in R_{cont}, R_{Cl-}, R_{Pb}, and R_{As} at the end of the experiment.
Explanations: Ep – epidermis; En – endodermis; Cortx – cortex; VC – vallecular canal; CC - carinal canal; PC – pith cavity; Sc – sclerenchyma. Control reactor (R_{cont}), chloride treated reactor (R_{Cl-}), lead treated reactor (R_{Pb}), and arsenic treated reactor (R_{As}). Scale bars 500 μm (a) and 250 μm (b). Red arrows/lines point out: a) disturbances in a septum (R_{Pb}) and elongation of VC in Cortx (R_{As}) and b) irregular CC formation (R_{Pb}).

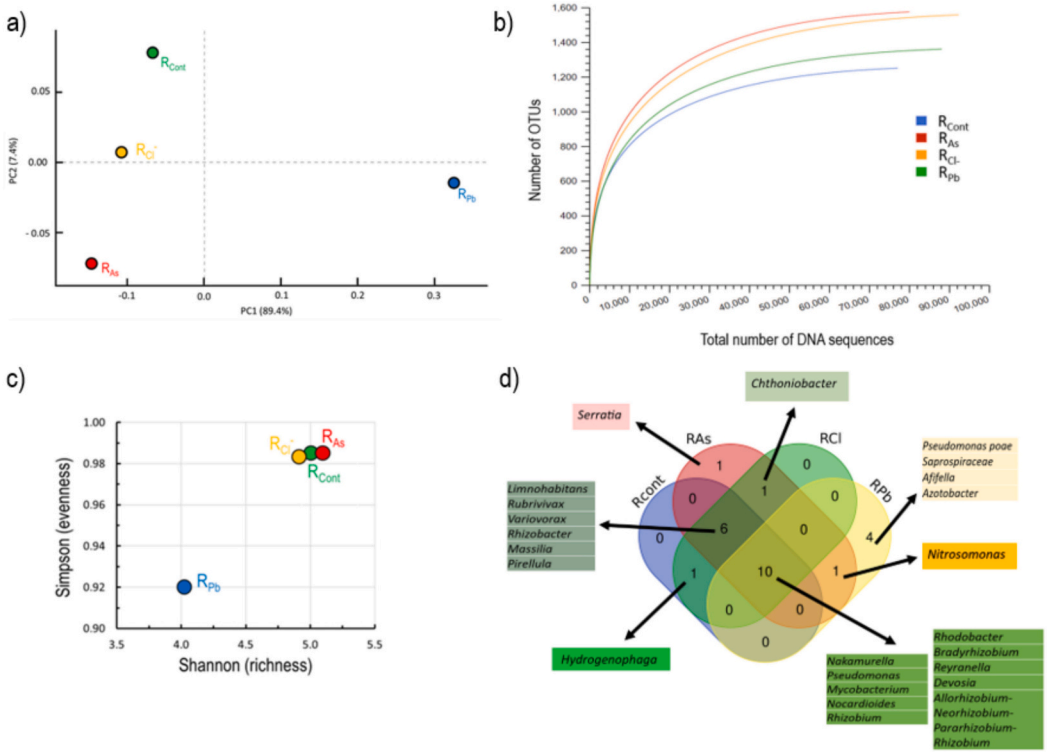

Fig. 5. Biodiversity and structure of the bacterial communities in the rhizosphere of the *E. hyemale* in the control reactor (R_{cont}) and in the reactors treated with As (R_{As}), Cl (R_{Cl}) and Pb (R_{Pb}) expressed as: a) PCA plot reflecting differences between bacterial community structure in samples from the tested reactors on phylum level, calculated with the ANOVA test in STAMP ($p < 0.05$) (b) rarefaction curves, (c) Shannon and Simpson diversity indices and (d) Venn diagram for the genera ≥0.8 % within total bacterial community

was 4.02 (Fig. 5c). Simpson index values proved relatively high evenness of the taxa in the R_{As}, R_{Cl-}, and R_{cont}, which reached 0.98 ± 0.01. In the R_{Pb}, the Simpson index value of 0.92 was visibly lower than the mean value from the all analysed cases 0.97 (SD ± 0.03), which suggests the predominance of the specified bacterial taxa within the total bacterial community.

Taxonomic data analysis identified 10 bacteria phyla which accounted for >1.5 % in total bacterial community. At the phylum level, the predominant bacteria belonged to the *Proteobacteria* (54.1 % ± 5.1 %) and *Actinobacteriota* (22.2 ± 3.4%). In the Pb treatment, the abundance of *Proteobacteria* was relatively high (61.8%), whereas the abundance of *Actinobacteriota* was relatively low (17.2 %). The averaged shares of the remaining *Phyla* were notably lower, ranging from 0.7 % to 5.3 % for the *Bacteroidota, Cyanobacteria*, *Planctomyceota, Acidobacteriota*, *Chloroflexi*, *Bdellovibrionota*, *Verrucomicrobiota* and *Firmicutes*.

The bacterial consortia showed greater variation in composition at the genus level between reactors. By considering shares ≥ 0.8 % within the total bacterial community, representatives of the ten genera (*Allorhizobium-Neorhizobium-Pararhizobium-Rhizobium, Bradyrhizobium, Devosia, Mycobacterium, Nakamurella, Nocardioides, Pseudomonas, Reyranella, Rhizobium, Rhodobacter*) constituted common component in all analysed reactors (Fig. 5d). In terms of other genera with shares ≥ 0.8 %, representatives of *Limnohabitans, Massilia, Pirellulafor, Rubrivivax, Rhizobacter, Variovorax* occurred mutually in control, salinity, and As treatment. However, their abundance was limited in Pb treatment.

The set of the predominant bacterial genera (≥ 0.8 %,) was most similar between control and salinity treatment. The most significant differences between R_{cont} and $R_{\bar{Cl}}$ were in the abundances of *Mycobacterium, Hydrogenophaga, Pseudomonas and Rhodoferax* (Fig. S.1). Under conditions of elevated chloride concentration the share of *Mycobacterium* was about twice as high (7.8 % vs. 3.9 %), while the contribution of *Hydrogenophaga, Pseudomonas and Rhodoferax* to the rhizomicrobiome was slightly reduced. Representatives of *Mycobacterium* are considered as a common and often predominant component of the microbiome of the plant roots (Wang et al., 2016). A study by Bouam et al. (2018) confirmed tolerance of *Mycobacterium* tolerance to NaCl concentrations ranging from 0 to 10 %, as well as versatile capability for hydrocarbons biodegradation, which enable them to colonize plant roots and promote plant growth, thus gain potential advantage over other bacterial groups under elevated salinity.

In the R_{Pb} four unique genera emerged over the experimental period including representatives of *Azotobacter, Afifella, Pseudomonas poae* and *Saprospiraceae*. Another specific feature of the rhizobiome in R_{Pb} was the noticeable reduction or even elimination of many bacterial genera such as *Bradyrhizobium, Hydrogenophaga, Limnohabitans, Massilia* or *Rhodoferax*, while on the other hand *Pseudomonas* and *Azotobacter,* both belonging to the phylum of the *Proteobacteria*, dominated the community with shares of 24.4 % and 10.7 % respectively. In the other treatments, no group achieved such advantage, which is consistent with the lowest biodiversity index for treatment $R_{Pb.}$

In treatment R_{As} similar patterns were observed for the R_{cont} rhizomicrobiome, i.e. *Mycobcaterium* showed higher abundance (6.2 %), while *Hydrogenophaga, Pseudomonas* and *Rhodoferax* were the genera with the most reduced occurrence.

3.5. Abundance of specific metabolic bacterial groups

Most of the identified bacterial groups represented typical heterotrophic (HET)/mixotrophic metabolism, with a preference for aerobic growth and capability for the decomposition of sugars and proteins (Table 3). Despite the presence of HET bacteria, canonical nitrifiers were found in all reactors. The most abundant ammonium oxidizing bacteria (AOB) groups were representatives of *Nitrosomonas*, which contributed 0.45 ± 0.04 % in the R_{cont}, $R_{\bar{Cl}}$ and 0.75 ± 0.12 % in the R_{Pb} and R_{As}. The second detected AOB genera was *Nitrosospira* with averaged share 0.25 ± 0.01 %. Nitrite oxidizing bacteria (NOB) were exclusive represented by genus *Nitrospira* (avg. 0.2 ± 0.01 %).

DNA sequences specified for nitrogen fixing bacteria were abundant components of the obtained 16S rRNA gene libraries. Members of three genera, *Allorhizobium-Neorhizobium-Pararhizobium-Rhizobium*, *Bradyrhizobium* and *Rubrivivax* were detected in all analysed systems. However, their shares were significantly lower in the reactor treated with Pb (SI data). This observation suggests that Pb toxicity disrupts the structure of the rhizobiome.

4. Discussion

None of the applied stress factors, i.e., increased salinity, presence of Pb, or presence of As, affected removal of total nitrogen (TN) in floating treatment wetland (FTW) microcosms planted with *E. hyemale*, suggesting that nitrogen removal pathways were not disturbed. Pavlineri et al. (2017) evaluated the effectiveness of 63 FTW systems in removing TN from wastewater. They reported an average TN removal efficiency of 58 % across the systems. In microcosm studies, *E. hyemale* FTW systems demonstrated effective TN removal capabilities. Arsenic presence adversely impacted PO_4-P.

4.1. Salinity

Salinity, commonly resulting from road salt application during frosts, does not hinder the nutrient removal performance of *E. hyemale* FTWs. In fact, elevated salt concentrations accelerated PO_4-P depletion compared to the control treatment, where PO_4-P began to decline after 25 days. Salt stress, caused both by sodium (Na^+) and chloride (Cl^-) ions, disrupts plant water balance in the short-term (osmotic stress), while long-term exposure leads to ion accumulation and phytotoxicity (Ebeed et al., 2024). Sodium (Na^+) ions compete with potassium (K^+) for uptake, while chloride (Cl^-) disrupts anion uptake (e.g. NO_3^- and PO_4^{3-}) in plants through antagonism (Massa et al., 2009). A balance of ions in the natural environment is essential for optimal plant growth and development. Ebeed et al. (2024) highlighted the beneficial role of silicon (Si) for plants under salt stress. In current short-term experiment, *E. hyemale* exhibited tolerance to salts (Fig. S.2).

Landaverde et al. (2024) examined the growth of saltmarsh plants in FTWs and discovered that species respond differently to salinity exposures; *Distichlis spicata* and *Juncus roemerianus* exhibited apparent inhibition of growth, whereas *Spartina alterniflora* and *Spartina patens* exhibited the highest biomass production when exposed to saline conditions. Schück and Greger (2022) established a correlation between chloride removal capacity and biomass, dry: fresh biomass ratio, water uptake, and transpiration of plants. Plant species employed for phytodesalination in hydroponic settings should remove at least 7 kg Cl^-/m^2 to be considered suitable candidates (Schück and Greger, 2022).

Similar bacterial structures in the control and salinity treatment indicate that elevated salt concentrations (800 mg/L Cl^- compared to 300 mg/L in other reactors, did not significantly impact bacterial community biodiversity or selection of the specified genera. Baldwin et al. (2006) obtained a similar finding in their assessment of short-term effects of salinization, ranging from 0 to 3545 mg/L, on bacterial community structure in freshwater wetland sediment. Their study only revealed minor differences in terminal restriction fragment length polymorphism (T-RFLP). In addition, Roeßler et al. (2003) demonstrated that a broad group of bacteria, including *Bacillus*, *Escherichia* and *Paracoccus* genera, can tolerate and maintain effective growth in chloride concentrations up to 28,360 mg/L (up to 53,173 mg/L in the case of *Proteus mirabilis)*.

4.2. Lead (Pb)

The most surprising outcome was observed in R_{Pb}, where the highest

nutrients removal efficiencies were achieved compared to all other treatments. The addition of Pb did not hinder nutrient removal processes and even seemed to accelerate them. This unexpected result is likely due to the changes in bacterial community structure observed in R_{Pb}. Lead was the most influential stress factor in terms of bacterial community composition, causing a significant reduction in biodiversity. However, it also favoured the development of certain taxa that are resistant to Pb toxicity. Two genera, *Pseudomonas* and *Azotobacter*, gained a competitive advantage over other bacterial groups in R_{Pb}. *Pseudmonas* and *Azotobacter* are both aerobic heterotrophs that are capable of carrying out denitrification.

Members of the genus *Pseudomonas* are known for their tolerance to elevated Pb concentrations, with some strains able to withstand 200 mg/L of Pb (Kalita and Joshi, 2017). *Pseudomonas* species are also characterized by their versatile metabolic capabilities, which enable them to adapt to even highly polluted environments and respond effectively to various physicochemical stresses. This allows them to outcompete over other bacterial groups (Weimer et al., 2020).

In terms of the Pb contamination, members of *Pseudomonas* synthesise and excrete rhamnolipid biosurfactants, which can sequester lead (Chen et al., 2021). Additionally, *Pseudomonas* species have a wide range of metabolic pathways that help them to respond to stress, such as expressing stress resistance proteins, altering their cell membrane composition, and trans-isomerization cell membrane phospholipids (Ramos et al., 2015). These adaptations allow them to survive in the toxic environment of treatment R_{Pb}.

Similar metabolic features were observed in *Azotobacter* bacteria, which showed a high capacity to biosorb Pb at concentrations as high as 250 mg/L (Dhevagi et al., 2021). The suppression of less resistant bacterial groups and the proliferation of Pb-tolerant *Pseudomonas* and *Azotobacter* species had a beneficial effect on nitrogen removal in treatment R_{Pb}.

The Pb(II) added as nitrate to the FTW reactors quickly adsorbs onto plant roots hanging in the water column or forms organic complexes in solution. The mass balance indicated that 50 % of Pb at the end of the first phase and 32 % of Pb at the end of the second phase was accumulated in the root biomass of *E. hyemale* (Fig. 2). That can be considered as a considerable accumulation. In comparison to another study (Nawrot et al., 2023) on treatment of chromium (Cr) in FTWs using *Phragmites australis* and *Iris pseudacorus*, the maximum percentage of Cr bound by plants was 19 and 22 %, respectively. Lead is generally taken up by plants passively and stored mainly in the roots (Kabata-Pendias and Pendias, 2001).

The response of *E. hyemale* to Pb stress is evident in micrographs of rhizomes, which show disturbance in a septum (marked with a red arrow in Fig. 4a) in R_{Pb}. This may be related to high Pb uptake by *E. hyemale*. Additionally, aerial stems in R_{Pb} showed irregular carinal canal formation. Anatomical changes in plant organs, such as changes in vascular tissues, are primarily induced by reduced cell elongation, restricted stimulation of cell division, and changes in cell differentiation circumstances under stresses. Stress causes the generation of reactive oxygen species (so called oxidative stress), resulting in growth retardation, altered photosynthetic apparatus, and changes in the ultrastructure of plant tissues, plasma membrane permeability, stomatal behaviour, etc. (Roychoudhury and Tripathi, 2019).

High and quick increase of Pb concentration in roots suggest that *E. hyemale* is effective for phytoaccumulation of Pb. This could be due to a high concentration of silicon (Si) in *E. hyemale* sp. tissues, as reported in the literature (Gierlinger et al., 2008; Sapei et al., 2007). Silicon and Pb belong to the same group of elements. In addition to monosilicic acid, monoplumbic acid is produced in the roots of Pb-exposed plants; this reaction intermediate is connected with Pb bioaccumulation (Pant et al., 2015). The results obtained in this study may indicate that the Si characteristic of the tissues of *E. hyemale* sp. plays a protective role in reducing the effects of abiotic stress, which was previously confirmed by Guerriero et al. (2016).

4.3. Arsenic (As)

The As treatment significantly impaired PO_4-P removal, while nitrogen removal efficiency was slightly higher than in R_{cont}. This could be due to the similar physiochemical characteristics of phosphate- and arsenate compounds, which lead to competition for uptake by plants (Anawar et al., 2018). According to Li et al. (2016), As(V) enters plant roots easily through phosphate transporters, whereas As(III) enters through aquaporins, which are membrane channels that transport water and small neutral molecules. In comparison to the initial As root concentration (0.28 ± 0.1 mg/kg d.w.), the concentration of As in the plant's roots increased to 20.3 ± 1.8 mg/kg d.w. at the end of the 1st phase and to 48.1 ± 2.1 mg/kg d.w. at the end of the 2nd. The change in concentration was evident, however the mass balance indicates that only 0.5 % of As was bound to plant root biomass at the end of both phases of the experiment (Fig. 2). This could be due to the duration of the experiment; short-term screening results (50 days) do not confirm *E. hyemale* as an As bioaccumulator. Other expected pathways for As removal that could not be quantified in this study include: 1) loss through washing roots at the end of the experiment; 2) binding by microorganisms and suspension deposited on the 0.45 μm filter during liquid sample collection; and 3) precipitation or sorbed on the reactor walls/bottom.

The As treatment appeared to have minor detrimental effects on *E. hyemale* plants. The relative growth rate observed in R_{As} was similar to those observed in R_{cont} and R_{Cl}. Also the chlorophyll content index was similar to R_{cont}, indicating that As had no further influence on plant condition. Only subtle tissue-level changes were observed in $R_{As,}$ with elongation of vallecular canal in the cortex with carinal canal regular formation.

Unlike in all other treatments, a unique *Serratia* subpopulation developed in R_{As}. The presence of *Serratia* is likely associated with its high tolerance to arsenate (almost 30,000 mg/L) and its ability to dissimilative arsenate reduction, as confirmed by Drewniak et al. (2014). Additionally, a study by Cheng et al. (2020) found that *Serratia liquefaciens* played a key role in immobilizing As in arsenic-contaminated soil, thereby reducing the toxic effects of As on plant growth. The potential synergy between *E. hyemale* and *Serratia* may play a crucial role in mitigating the adverse effects of As to plants, as evidenced by the minimal effects of As on elongation of the vallecular canals as mentioned above.

Besides the genus *Serratia,* the ability to oxidize As(III) to As(V) has been identified for a number of other bacteria, such as *Achromobacter*, *Acinetobacter*, *Alcaligenes*, *Bacillus*, *Klebsiella*, *Lysinibacillus*, *Pseudomonas*, where, compared to As(III), As(V) shows less toxicity and has a strong affinity for particulate matter such as iron and manganese oxides. This affinity limits the migration of As(V) in the environment and reduces its bioavailability to other organisms, including plants (He et al., 2023). Arsenic resistance and transformation in mentioned bacterial groups are attributed to their detoxification mechanisms, regulated by correlated genes such as *aio*, *arr*, and *ars* (Badilla et al., 2018). For instance He et al. (2023) identified high accumulation capacity (up to 2977 mg/g) of As by the *Pseudomonas* sp. SMS11 strain, which effectively removed As from the liquid solution. Therefore, the low As content in the liquid phase observed in this study should be linked to the potential bioaccumulation of As in the bacterial biomass/biofilm deposited in the reactor. Overall, 21 and 26 % of As remained in solution at the end of phases 1 and 2, and over 78 and 73 % of As was removed by another removal route. Microorganisms may have been significant in this case, although they might have been efficiently retained by filtering liquid samples with a 0.45 um filter size (part of the filter was not retrieved).

5. Conclusions

This study investigated the performance of nutrient removal in a FTW with *E. hyemale* under the influence of abiotic stressors, namely

salinity, Pb, and As during a short-term screening period spanning 50 days divided into 2 phases. The findings affirm that *E. hyemale* robustly supports nitrogen removal in FTW applications, even under unfavorable conditions induced by the addition of As, Pb, and elevated salinity levels. Notably, *E. hyemale* efficiently removed phosphate-phosphorus (PO_4-P) except when As was present. The chemical similarity between phosphate and arsenate likely led to competition for uptake sites within the plants.

The study further revealed that FTWs with *E. hyemale* effectively removed lead (Pb) and arsenic (As), achieving removal rates as high as 98 % for Pb and 79 % for As. Interestingly, chloride (Cl^-) treatment did not hinder nutrient removal or harm plant health, indicating *E. hyemale*'s tolerance to chloride. The significant accumulation of Pb in plant material (reaching 51 % and 33 % at the end of first and second phases, respectively) highlights *E. hyemale*'s potential as a Pb bioaccumulator, although stress-induced disruptions were observed at the tissue level.

Furthermore, the high silicon (Si) content in *E. hyemale* might effectively mitigate stress from toxic Pb, making it an even more attractive choice for FTWs applications. While As treatments led to a substantial decrease in aqueous As concentration, low absorption and binding in biomass suggests limited uptake by plants. Notably, Pb exposure had a more pronounced effect on *E. hyemale* than As, impacting both its growth and microscopic features more strongly than in the As treatment.

The different treatments significantly impacted the rhizobiome within the FTWs. The salinity treatment resembled the control group, while the As treatment fostered a unique *Serratia* subpopulation with high tolerance and arsenate-reducing capabilities. However, it also led to a decrease in *Hydrogenophaga, Pseudomonas*, and *Rhodoferax* populations. Pb exposure had the most dramatic effect, reducing overall bacterial biodiversity and eliminating specific genera. However, it also promoted tolerant groups like *Pseudomonas* and *Azotobacter*, whose dominance as heterotrophic denitrifiers likely explains the observed high nitrogen removal rates observed in the Pb treatment. In conclusion, *E. hyemale* demonstrated suitability for FTW applications due to its resilience to abiotic stressors and efficient uptake of Pb and As.

CRediT authorship contribution statement

Nicole Nawrot: Writing – review & editing, Writing – original draft, Visualization, Resources, Project administration, Methodology, Investigation, Funding acquisition, Formal analysis, Data curation, Conceptualization. **Przemysław Kowal:** Writing – review & editing, Writing – original draft, Methodology, Investigation, Conceptualization. **Ewa Wojciechowska:** Writing – review & editing, Writing – original draft, Supervision. **Ksenia Pazdro:** Writing – review & editing, Supervision. **Jolanta Walkusz-Miotk:** Validation, Methodology. **Sławomir Ciesielski:** Writing – review & editing, Supervision. **Filip M.G. Tack:** Writing – review & editing, Supervision.

Declaration of competing interest

The authors declare the following financial interests/personal relationships which may be considered as potential competing interests: Nicole Nawrot reports financial support was provided by National Science Centre Poland under the Preludium 18 research project [2019/35/N/ST8/01134] – beneficiary of the funds: Nicole Nawrot.

If there are other authors, they declare that they have no known competing financial interests or personal relationships that could have appeared to influence the work reported in this paper.

Data availability

Data available: https://doi.org/10.34808/t9a7-yz17

Floating treatment wetland with Equisetum hyemale - performance in nutrients and potentially toxic elements removal (Original data) (Bridge of Knowledge)

Acknowledgements

This work was financed by the National Science Centre, Poland under the Preludium 18 research project [2019/35/N/ST8/01134] – beneficiary of the funds: Nicole Nawrot.

Appendix A. Supplementary data

Supplementary data to this article can be found online at https://doi.org/10.1016/j.scitotenv.2024.174468.

References

Anawar, H.M., Rengel, Z., Damon, P., Tibbett, M., 2018. Arsenic-phosphorus interactions in the soil-plant-microbe system: dynamics of uptake, suppression and toxicity to plants. Environ. Pollut. 233, 1003–1012. https://doi.org/10.1016/j.envpol.2017.09.098.

Badilla, C., Osborne, T.H., Cole, A., Watson, C., Djordjevic, S., Santini, J.M., 2018. A new family of periplasmic-binding proteins that sense arsenic oxyanions. Sci. Rep. 8 (1) https://doi.org/10.1038/s41598-018-24591-w.

Baldwin, D.S., Rees, G.N., Mitchell, A.M., et al., 2006. The short-term effects of salinization on anaerobic nutrient cycling and microbial community structure in sediment from a freshwater wetland. Wetlands 26, 455–464. https://doi.org/10.1672/0277-5212(2006)26[455:TSEOSO]2.0.CO;2.

Borne, K.E., Tanner, C.C., Fassman-beck, E.A., 2013. Stormwater nitrogen removal performance of a floating treatment wetland. Water Sci. Technol. 1657–1664 https://doi.org/10.2166/wst.2013.410.

Bouam, A., Armstrong, N., Levasseur, A., Drancourt, M., 2018. Mycobacterium terramassiliense, Mycobacterium rhizamassiliense and Mycobacterium numidiamassiliense sp. nov., three new Mycobacterium simiae complex species cultured from plant roots. Sci. Rep. 8 (1) https://doi.org/10.1038/s41598-018-27629-1.

Cannon, H.L., Shacklette, H.T., Bastron, H., 1968. Metal absorption by Equisetum (Horsetail). United States: N. p., 1968. Web.

Chemat, Z., Hadj-Boussaad, D.E., Chemat, F., 1998. Application of atmospheric pressure microwave digestion to total Kjeldahl nitrogen determination in pharmaceutical, agricultural and food products. Analusis 26 (5), 205–209.

Chen, Q., Li, Y., Liu, M., Zhu, B., Mu, J., Chen, Z., 2021. Removal of Pb and Hg from marine intertidal sediment by using rhamnolipid biosurfactant produced by a Pseudomonas aerugino- sa strain. Environ. Technol. Innov. 22 https://doi.org/10.1016/j.eti.2021.101456.

Cheng, C., Nie, Z.W., He, L.Y., Sheng, X.F., 2020. Rice-derived facultative endophytic Serratia liquefaciens F2 decreases rice grain arsenic accumulation in arsenic-polluted soil. Environ. Pollut. 259 https://doi.org/10.1016/j.envpol.2019.113832.

Colares, G.S., Dell'Osbel, N., Wiesel, P.G., Oliveira, G.A., Lemos, P.H.Z., da Silva, F.P., Lutterbeck, C.A., Kist, L.T., Machado, Ë.L., 2020. Floating treatment wetlands: a review and bibliometric analysis. Sci. Total Environ. 714, 136776 https://doi.org/10.1016/j.scitotenv.2020.136776.

Dhevagi, P., Priyatharshini, S., Ramya, A., Sudhakaran, M., 2021. Biosorption of lead ions by exopolysaccharide producing Azotobacter sp. J. Environ. Biol. 42 (1), 40–50. https://doi.org/10.22438/JEB/42/1/MRN-1231.

Drewniak, L., Rajpert, L., Mantur, A., Sklodowska, A., 2014. Dissolution of arsenic minerals mediated by dissimilatory arsenate reducing bacteria: estimation of the physiological potential for arsenic mobilization. Biomed. Res. Int. 2014 https://doi.org/10.1155/2014/ 841892.

Ebeed, H.T., Ahmed, H.S., Hassan, N.M., 2024. Silicon transporters in plants: unravelling the molecular Nexus with sodium and potassium transporters under salinity stress. Plant Gene 38. https://doi.org/10.1016/j.plgene.2024.100453.

Gao, X., Lee, J.R., Park, S.K., Kim, N.G., Choi, H.G., 2018. Detrimental Effects of Sediment on Attachment, Survival and Growth of the Brown Alga Sargassum Thunbergii in Early Life Stages. September. https://doi.org/10.1111/pre.12347.

Geng, Y., Han, W., Yu, C., Jiang, Q., Wu, J., Chang, J., Ge, Y., 2017. Effect of plant diversity on phosphorus removal in hydroponic microcosms simulating floating constructed wetlands. Ecol. Eng. 107, 110–119. https://doi.org/10.1016/j.ecoleng.2017.06.061.

Gierlinger, N., Sapei, L., Paris, O., 2008. Insights into the chemical composition of Equisetum hyemale by high resolution Raman imaging. Planta 227 (5), 969–980. https://doi.org/10.1007/s00425-007-0671-3.

Guerriero, G., Hausman, J.F., Legay, S., 2016. Silicon and the plant extracellular matrix. In: Frontiers in Plant Science, Vol. 7, Issue APR2016. Frontiers Media S.A. https://doi.org/10.3389/fpls. 2016.00463.

He, X., Xiao, W., Zeng, J., Tang, J., Wang, L., 2023. Detoxification and removal of arsenite by Pseudomonas sp. SMS11: oxidation, biosorption and bioaccumulation. J. Environ. Manag. 336 https://doi.org/10.1016/j.jenvman.2023.117641.

Higbie, S.M., Wang, F., Stewart, J. McD, Sterling, T.M., Lindemann, W.C., Hughs, E., Zhang, J., 2010. Physiological response to salt (NaCl) stress in selected cultivated tetraploid cottons. Int. J. Agron. 2010, 1–12. https://doi.org/10.1155/2010/643475.

Kabata-Pendias, A., Pendias, H., 2001. Biogeochemistry of trace elements. Trace elements in soils and plants, fourth edition (vol. 2nd) chapter 5 (trace elements in plants).
Kalita, D., Joshi, S.R., 2017. Study on bioremediation of Lead by exopolysaccharide produ- cing metallophilic bacterium isolated from extreme habitat. Biotechnology Reports 16, 48–57. https://doi.org/10.1016/j.btre.2017.11.003.
Klindworth, A., Pruesse, E., Schweer, T., Peplies, J., Quast, C., Horn, M., Glöckner, F.O., 2013. Evaluation of general 16S ribosomal RNA gene PCR primers for classical and next-generation sequencing-based diversity studies. Nucleic Acids Res. 41 (1) https://doi.org/10.1093/nar/gks808.
Kowal, P., Mehrani, M.J., Sobotka, D., Ciesielski, S., Mąkinia, J., 2022. Rearrangements of the nitrifiers population in an activated sludge system under decreasing solids retention times. Environ. Res. 214 https://doi.org/10.1016/j.envres.2022.113753.
Landaverde, A.C., Strosnider, W.H.J., White, S.A., 2024. Plant suitability for floating treatment wetland applications in brackish waters. Ecol. Eng. 200, 107183 https://doi.org/10.1016/j.ecoleng.2024.107183.
Li, N., Wang, J., Song, W.Y., 2016. Arsenic uptake and translocation in plants. In: Plant and Cell Physiology, Vol. 57, Issue 1. Oxford University Press, pp. 4–13. https://doi.org/10.1093/pcp/pcv143.
Ling, Q., Huang, W., Jarvis, P., 2011. Use of a SPAD-502 meter to measure leaf chlorophyll concentration in Arabidopsis thaliana. Photosynth. Res. 107 (2), 209–214. https://doi.org/10.1007/s11120-010-9606-0.
Liu, X., Ju, Y., Mandzhieva, S., Pinskii, D., Minkina, T., Rajput, V.D., Roane, T., Huang, S., Li, Y., Ma, L.Q., Clemens, S., Rensing, C., 2023. Sporadic Pb accumulation by plants: influence of soil biogeochemistry, microbial community and physiological mechanisms. In: Journal of Hazardous Materials, Vol. 444. Elsevier B.V. https://doi.org/10.1016/j.jhazmat.2022.130391.
Marschner, H., 2012. Mineral Nutrition of Higher Plants Third Edition (3rd ed.).
Massa, D., Mattson, N.S., Lieth, H.J., 2009. Effects of saline root environment (NaCl) on nitrate and potassium uptake kinetics for rose plants: a Michaelis-Menten modelling approach. Plant and Soil 318 (1–2), 101–115. https://doi.org/10.1007/s11104-008-9821-z.
Mohsin, M., Nawrot, N., Wojciechowska, E., Kuittinen, S., Szczepańska, K., Dembska, G., Pappinen, A., 2023. Cadmium accumulation by Phragmites australis and Iris pseudacorus from stormwater in floating treatment wetlands microcosms: insights into plant tolerance and utility for phytoremediation. J. Environ. Manage. 331, 117339 https://doi.org/10.1016/j.jenvman.2023.117339.
Nawrot, N., Wojciechowska, E., Mohsin, M., Kuittinen, S., Pappinen, A., Matej-Łukowicz, K., Szczepańska, K., Cichowska, A., Irshad, M.A., Tack, F.M.G., 2023. Chromium (III) removal by perennial emerging macrophytes in floating treatment wetlands. Sci. Rep. 13 (1) https://doi.org/10.1038/s41598-023-49952-y.
Pant, D., Sharma, V., Singh, P., 2015. Pb detoxification in Equisetum diffusum. Toxicol. Rep. 2, 716–720. https://doi.org/10.1016/j.toxrep.2015.04.006.
Parker, A.J., Haskins, E.F., Deyrup-Olsen, I., 1982. Toluidine blue: a simple, effective stain for plant tissues. Am. Biol. Teach. 44 (8), 487–489. https://doi.org/10.2307/4447575.
Parks, D.H., Beiko, R.G., 2010. Identifying biologically relevant differences between metagenomic communities. Bioinformatics 26 (6), 715–721. https://doi.org/10.1093/bioinformatics/ btq041.
Pavlineri, N., Skoulikidis, N.T., Tsihrintzis, V.A., 2017. Constructed floating wetlands: a review of research, design, operation and management aspects, and data meta-analysis. Chem. Eng. J. 308, 1120–1132. https://doi.org/10.1016/j.cej.2016.09.140.
Ramos, J.L., Cuenca, M.S., Molina-Santiago, C., Segura, A., Duque, E., Ǵomez-Garciá, M. R., Udaondo, Z., Roca, A., 2015. Mechanisms of solvent resistance mediated by interplay of cellular factors in Pseudomonas putida. In: FEMS Microbiology Reviews, Vol. 39, Issue 4. Oxford University Press, pp. 555–566. https://doi.org/10.1093/femsre/fuv006.
Roeßler, M., Sewald, X., Müller, V., 2003. Chloride dependence of growth in bacteria. FEMS Microbiol. Lett. 225 (1), 161–165. https://doi.org/10.1016/S0378-1097(03)00509-3.
Roychoudhury, Aryadeep, Tripathi, D. Kumar, 2019. Plant Abiotic Stress: Molecular Biology and Biotechnological Advances. Wiley.
Sapei, L., Gierlinger, N., Hartmann, J., Nöske, R., Strauch, P., Paris, O., 2007. Structural and analytical studies of silica accumulations in Equisetum hyemale. Anal. Bioanal. Chem. 389 (4), 1249–1257. https://doi.org/10.1007/s00216-007-1522-6.
Schück, M., Greger, M., 2022. Chloride removal capacity and salinity tolerance in wetland plants. J. Environ. Manage. 308 https://doi.org/10.1016/j.jenvman.2022.114553.
Spinedi, N., Rojas, N., Storb, R., Cabrera, J., Aranda, E., Salierno, M., Svriz, M., Scervino, J.M., 2019. Exploring the response of Marchantia polymorpha: growth, morphology and chlorophyll content in the presence of anthracene. Plant Physiol. Biochem. 135 (July), 570–574. https://doi.org/10.1016/j.plaphy.2018.11.001.
Walkowiak, R., 2018. Equisetum hyemale, 25.12.17. Technical Report, January. https://doi.org/10.13140/RG.2.2.18709.42726.
Wang, W., Zhai, Y., Cao, L., Tan, H., Zhang, R., 2016. Illumina-based analysis of core actinobacteriome in roots, stems, and grains of rice. Microbiol. Res. 190, 12–18. https://doi.org/10.1016/j.micres.2016.05.003.
Wang, Y., Sun, B., Gao, X., Li, N., 2019. Development and evaluation of a process-based model to assess nutrient removal in floating treatment wetlands. Sci. Total Environ. 694 (August) https://doi.org/10.1016/j.scitotenv.2019.133633.
Weimer, A., Kohlstedt, M., Volke, D.C., Nikel, P.I., Wittmann, C., 2020. Industrial biotech- nology of Pseudomonas putida: advances and prospects. In: Applied Microbiology and Biotechnology, Vol. 104, Issue 18. Springer, pp. 7745–7766. https://doi.org/10.1007/s00253-020-10811-9.
Yang, Y., Zhang, L., Huang, X., Zhou, Y., Quan, Q., Li, Y., Zhu, X., 2020. Response of photosynthesis to different concentrations of heavy metals in Davidia involucrata. PloS One 15 (3). https://doi.org/10.1371/journal.pone.0228563.
Yasin, M., Tauseef, M., Zafar, Z., Rahman, M., Islam, E., Iqbal, S., Afzal, M., 2021. Plant-microbe synergism in floating treatment wetlands for the enhanced removal of sodium dodecyl sulphate from water. Sustain 13, 1–11. https://doi.org/10.3390/su13052883.
Koch, I., Hnain, A.K., Nearing, M., Weber, K.P., 2022. Uptake and speciation of arsenic in hydroponically exposed horsetail plants (Equisetum sp.). SSRN: https://doi.org/10.2139/ssrn.4255534.